NIH Public Access
Author Manuscript
Basic Res Cardiol. Author manuscript; available in PMC 2013 June 11.

Published in final edited form as:
Basic Res Cardiol. 2013 May ; 108(3): 348. doi:10.1007/s00395-013-0348-y.

Deletion of the last five C-terminal amino acid residues of connexin43 leads to lethal ventricular arrhythmias in mice without affecting coupling via gap junction channels

Indra Lübkemeier,
Life and Medical Sciences (LIMES) Institute, Molecular Genetics, University of Bonn, Carl-Troll-Str. 31, 53115 Bonn, Germany

Robert Pascal Requardt,
Center for Sepsis Control and Care (CSCC), Jena University Hospital, Jena, Germany

Xianming Lin,
Leon H. Charney Division of Cardiology, New York University Medical School, New York, NY, USA

Philipp Sasse,
Institute of Physiology I, Life and Brain Center, University of Bonn, Bonn, Germany

René Andrié,
Institute of Medicine-Cardiology, University of Bonn, Bonn, Germany

Jan Wilko Schrickel,
Institute of Medicine-Cardiology, University of Bonn, Bonn, Germany

Halina Chkourko,
Leon H. Charney Division of Cardiology, New York University Medical School, New York, NY, USA

Feliksas F. Bukauskas,
Dominick P. Purpura Department of Neuroscience, Albert Einstein College of Medicine, New York, NY, USA

Jung-Sun Kim,
Department of Pathology, Samsung Medical Center, Sungkyunkwan University School of Medicine, Seoul, Korea

Marina Frank,
Life and Medical Sciences (LIMES) Institute, Molecular Genetics, University of Bonn, Carl-Troll-Str. 31, 53115 Bonn, Germany

Daniela Malan,
Institute of Physiology I, Life and Brain Center, University of Bonn, Bonn, Germany

Jiong Zhang,
Institute of Cellular Neurosciences, University of Bonn, Bonn, Germany

© Springer-Verlag Berlin Heidelberg 2013

Correspondence to: Klaus Willecke.

M. Delmar and K. Willecke contributed equally to this work.

Electronic supplementary material The online version of this article (doi:10.1007/s00395-013-0348-y) contains supplementary material, which is available to authorized users.

Conflict of interest The authors declare that they have no conflict of interest.

NIH-PA Author Manuscript
NIH-PA Author Manuscript
NIH-PA Author Manuscript

NIH-PA Author Manuscript

NIH-PA Author Manuscript

NIH-PA Author Manuscript

Angela Wirth,
Max Planck Institute for Heart and Lung Research, Bad Nauheim, Germany

Radoslaw Dobrowolski,
Department of Biological Sciences, Rutgers University, Newark, NJ, USA

Peter J. Mohler,
Departments of Internal Medicine and Physiology, Dorothy M. Davis Heart and Lung Research Institute, Ohio State University Medical Center, Columbus, OH, USA

Stefan Offermanns,
Max Planck Institute for Heart and Lung Research, Bad Nauheim, Germany

Bernd K. Fleischmann,
Institute of Physiology I, Life and Brain Center, University of Bonn, Bonn, Germany

Mario Delmar, and
Leon H. Charney Division of Cardiology, New York University Medical School, New York, NY, USA

Klaus Willecke
Life and Medical Sciences (LIMES) Institute, Molecular Genetics, University of Bonn, Carl-Troll-Str. 31, 53115 Bonn, Germany k.willecke@uni-bonn.de

Abstract

The cardiac intercalated disc harbors mechanical and electrical junctions as well as ion channel complexes mediating propagation of electrical impulses. Cardiac connexin43 (Cx43) co-localizes and interacts with several of the proteins located at intercalated discs in the ventricular myocardium. We have generated conditional Cx43D378stop mice lacking the last five C-terminal amino acid residues, representing a binding motif for zonula occludens protein-1 (ZO-1), and investigated the functional consequences of this mutation on cardiac physiology and morphology. Newborn and adult homozygous Cx43D378stop mice displayed markedly impaired and heterogeneous cardiac electrical activation properties and died from severe ventricular arrhythmias. Cx43 and ZO-1 were co-localized at intercalated discs in Cx43D378stop hearts, and the Cx43D378stop gap junction channels showed normal coupling properties. Patch clamp analyses of isolated adult Cx43D378stop cardiomyocytes revealed a significant decrease in sodium and potassium current densities. Furthermore, we also observed a significant loss of $Na_v1.5$ protein from intercalated discs in Cx43D378stop hearts. The phenotypic lethality of the Cx43D378stop mutation was very similar to the one previously reported for adult Cx43 deficient (Cx43KO) mice. Yet, in contrast to Cx43KO mice, the Cx43 gap junction channel was still functional in the Cx43D378stop mutant. We conclude that the lethality of Cx43D378stop mice is independent of the loss of gap junctional intercellular communication, but most likely results from impaired cardiac sodium and potassium currents. The Cx43D378stop mice reveal for the first time that Cx43 dependent arrhythmias can develop by mechanisms other than impairment of gap junction channel function.

Keywords

Connexin43; Zonula occludens protein-1; $Na_v1.5$; Intercalated disc

Introduction

Intercellular communication is essential for proper spread of excitation in the mammalian heart and is therefore required for normal cardiac function. In the adult ventricular

NIH-PA Author Manuscript

NIH-PA Author Manuscript

NIH-PA Author Manuscript

myocardium, protein complexes relevant to mechanical and electrical coupling are located at the end-to-end contact sites between cardiomyocytes, forming a specialized structure called the intercalated disc [12, 18]. Also resident in the intercalated disc is the complex of proteins that forms the voltage-gated sodium channel, primarily responsible for the excitatory current in most adult cardiac myocytes [43]. For years, molecules localized at the intercalated disc were thought to exist independently of each other. Recent studies have challenged this notion. Decreased N-Cadherin abundance affects $K_V1.5$ channels [7] and disruption of desmosomes or mixed adherens junctions decreases gap junction plaque abundance [2, 33]. Loss of Plakophilin 2 (PKP2) expression in cardiac cells leads to decreased amplitude and changed kinetics of the sodium current [49, 50]. These and several other examples (see [10–12] for review) lead to the concept that the intercalated disc is not a random assembly of separate proteins, but a subcellular domain where proteins interact to maintain intercellular communication and impulse propagation.

There is ample evidence demonstrating that expression and function of Cx43 is essential to normal cardiac rhythm. Loss or redistribution of Cx43 (so-called “gap junction remodeling”) has been associated with a number of pathologic conditions (see, e.g. [16, 42, 47]). Recent studies show that loss of Cx43 expression leads to a significant decrease in the amplitude of the sodium current, and changes in repolarizing currents [9, 13, 26]. However, dissecting the impact of gap junction-independent functions of Cx43 on cardiac electrophysiology has been impaired by the lack of an experimental model where coupling is preserved but Cx43-dependent interactions can still be investigated.

In this study, we have generated a novel transgenic mouse mutant (Cx43D378stop mice) which expresses a truncated form of the Cx43 gene lacking the last five C-terminal amino acid residues (DDLEI) of the protein. It has been previously shown in transfected cells that region 378–382 of Cx43 is important for interaction between Cx43 and its scaffolding protein zonula occludens-1 (ZO-1) [19, 24, 54]. ZO-1 co-localizes with Cx43 at the intercalated discs in the myocardium [4]. Our data show that ablation of this region leads to the occurrence of severe ventricular arrhythmias and sudden arrhythmic death in all Cx43D378stop mice. This is very similar to the phenotype previously reported for Cx43 deficient animals (Cx43KO; i.e. see [15]). However, in contrast to Cx43-KO animals, gap junction plaques are retained and remain functional in Cx43D378stop mice. As such, in Cx43D378stop mice, arrhythmic events are unlikely to be consequent to the loss of intercellular gap junction channels. Our results challenge the prevailing notion that, in the structurally normal heart, Cx43 dependent arrhythmias are due exclusively to loss of gap junction channels between cells. Our data provide novel mechanistic insight on the role of Cx43 in cardiac electrophysiology.

Methods

Methods are summarized in this section. Details are found in Online Resource 1

Construction of the conditional Cx43D378stop-vector—After generation of the Cx43D378stop mutation by PCR, the conditional Cx43D378stop vector was cloned in several steps (see Online Resource 1). The final conditional Cx43D378stop-vector contained the 5′ homologous region of Cx43 followed by loxP (locus of crossing over P1) sites flanking the Cx43 wild-type gene together with the 3′ untranslated region and the inverted neomycin resistance gene driven by a phosphoglycerate kinase (PGK) promoter and flanked by Flp recognition target (frt) sites. Downstream of the loxP-flanked region, we inserted the Cx43D378stop mutation followed by an IRES-eGFP sequence and the corresponding 3′ homologous region. The final Cx43D378stop exchange vector was analyzed by restriction mapping and partial sequencing (AGOWA, Berlin, Germany).

NIH-PA Author Manuscript

NIH-PA Author Manuscript

NIH-PA Author Manuscript

Screening of ES cell clones—For transfection of HM1 ES cells via electroporation, the conditional Cx43D378stop-vector was linearized by NotI digestion. Screening of positively transfected ES cells was carried out with 350 μg/μl G418-neomycin (Invitrogen, Darmstadt, Germany). Surviving ES cell clones were tested by PCR and by Southern blot hybridization with internal and external probes for correct recombination (see Online Resource 1).

Generation of Cx43D378stop mice—Two homologously recombined ES cell clones were injected into C57BL/6 blastocysts. Resulting high-extent fur-colored chimeras were bred with C57BL/6 mice and agouti-colored offspring genotyped. Heterozygous Cx43+/floxD378stop mice were backcrossed several times to increase C57BL/6 genetic background to at least 87.5 %. In addition, Cx43 +/floxD78stop mice were mated to Cre-recombinase (αMyHC- [1] and αMyHC-Cre-ER(T2) [55]) expressing mice to delete the wild-type Cx43 cDNA sequence and the neomycin resistance gene via the Cre/loxP system. After Cre mediated deletion of the Cx43 wild-type region, Cx43D378stop is expressed. Homologous recombination in floxed Cx43D78stop transgenic mice was verified by Southern blot analyses. Further details are seen in the Online Resource 1.

Intraperitoneal injection of tamoxifen dissolved in sterile peanut oil with 10 % ethanol was performed on four consecutive days at a dose of 3 mg each day. We used either heterozygous or homozygous Cx43floxD378stop mice as control mice. Adult control mice were injected with sterile peanut oil without tamoxifen.

All animal experiments were performed according to the Guidelines for the Care and Use of Laboratory Animals published by the US National Institutes of Health, and were approved by the local ethics committee.

Northern blot analyses—Hearts from newborn as well as adult Cx43D378stop and control mice were shock-frozen in liquid nitrogen. Total RNA was extracted using Trizol. After electrophoresis in an agarose gel, RNA was transferred on Hybond-N-membranes (Amersham Biosciences, Buck, UK). Hybridization was performed in Quick-Hyb solution (Stratagene, La Jolla, CA, USA) at 68 °C for 2 h.

Histological analyses—Hearts were shock-frozen in liquid nitrogen and cryosectioned (12 μm). For paraffin sections, hearts were directly fixed in 4 % paraformaldehyde after dissection, embedded after dehydration and sectioned (5 μm). Staining was performed with hematoxylin and eosin.

Surface-ECG recordings in ED 16.5 embryos—Embryos together with placenta were removed from the uterus, placed in a recording chamber and superfused with oxygenated tyrode solution at 33 ± 2 °C. Bipolar ECG was recorded by two silver chloride electrodes placed at the right and left chest wall with a bioamplifier recording system (PowerLab 8/35, AD instruments). Analysis of PQ and QRS duration was performed using the ECG analysis plugin of Chart (AD instruments).

Holter ECG: chip implantation and long-term ECG recording—Telemetric ECG recordings were performed with conscious tamoxifen-injected Cx43D378stop:αMyHC-Cre-ER(T2) and control mice using commercially available equipment (Data Science International, St. Paul, USA). Chips were implanted 10 days after the final tamoxifen injection. Recordings were obtained continuously until the death of the mice ($n = 4$), or in case of uninduced controls ($n = 4$), for 14 days. Data were sampled and stored digitally using standard equipment. All recordings were manually screened for spontaneous tachy- and bradyarrhythmias and alterations of the QRS-complex.

NIH-PA Author Manuscript

NIH-PA Author Manuscript

NIH-PA Author Manuscript

Langendorff-perfused hearts and epicardial mapping—Analysis of epicardial conduction was carried out in Langendorff-perfused adult hearts using a custom-built 128-electrode array (interelectrode distance: 300 ± 7 μm). Hearts were extracted from the mice 12 days after last tamoxifen injection, as described in [51]. Hearts were excorporated and dissected from surrounding tissue in ice-cold Krebs–Henseleit buffer. After cannulation of the aorta, hearts were retrogradely perfused in a Langendorff-apparatus (Radnoti Technologies Inc., Monrovia, CA, USA) at constant pressure perfusion (80 mmHg). All recordings were obtained at constant temperature (37 °C). Fixed-rate stimulation (S1S1 120 ms) was performed using two adjacent electrodes of the array. Electrograms were recorded using a 128-channel, computer-assisted recording system (Multi Channel Systems, Reutlingen, Germany) with a sampling rate of 25 kHz (25.000 samples per second). Data were bandpass filtered (50 Hz), digitized with 12 bit and a signal range of 20 mV. Activation maps were calculated using custom-programmed software (Labview 7.1, National Instruments, Austin, TX, USA). To obtain an index of local conduction slowing for each electrode, the activation time differences to neighboring points were normalised to interelectrode distance. The largest difference at each site was defined as local phase delay. The variation coefficient of these phase delays was used as heterogeneity index for inhomogeneity in global conduction, as described before [32, 51].

Microinjection analyses of cardiomyocytes—For dye coupling analysis, cardiomyocytes were isolated from the ventricles of embryonic hearts on ED 16.5, as described previously [21]. Cells from each heart were plated separately and the corresponding genotype was determined by PCR analysis of the embryonic tissue. The cardiomyocytes were injected at the periphery of beating clusters. The neurobiotin solution also contained rhodamine 3-isothiocyanate dextran, which cannot pass gap junctions. At least 20 injections were performed and analyzed. After the last injection, cells were fixed, washed, permeabilized and then incubated in 0.1 % horseradish peroxidase-conjugated Avidin D. After staining, neurobiotin-positive areas were evaluated under the microscope.

Cell-to-cell dye transfer and electrical coupling studies in Cx43D378stop HeLa cells—Coupling-deficient HeLa cells were stably transfected with a vector construct containing the Cx43D378stop-IRES-eGFP coding sequence under the control of a cytomegalovirus (CMV) promoter. To assess single channel permeability ($P\gamma$), we combined dye transfer studies with junctional conductance measurements, as described before [44]. Dyes used include (molecular mass of the fluorescent ion, valence): Lucifer yellow (LY) (443, –2), Alexa Fluor-350 (AF350) (326, –1), EAM-1 (MW 266, +1) and EAM-2 (MW 310, +1). Junctional conductance (g_j) was measured by dual whole-cell voltage clamp, as described previously [44].

Myocyte isolation and cell electrophysiology of Cx43D378stop cardiomyocytes—Adult mouse ventricular myocytes were obtained by enzymatic dissociation following standard procedures [40]. Ventricles were cut into small pieces, and gently minced. Ca^{2+} concentration was increased gradually to normal values. Cells were used for electrophysiological recording within 8 h after isolation.

All electrophysiological recordings were conducted in whole-cell configuration at room temperature, using standard protocols (detailed in Online Resource 1). Statistical tests were performed using unpaired Student's *t* test for all data. A *P*-value of <0.05 was considered significant. All data are expressed as mean ± SEM.

Immunochemical analyses for Cx43, ZO-1, N-Cadherin and $Na_v1.5$—Immunohistological analysis was carried out in cryosections obtained from adult

NIH-PA Author Manuscript

NIH-PA Author Manuscript

NIH-PA Author Manuscript

Cx43D378stop:αMyHC-Cre-ER(T2) and control hearts (14 days after last tamoxifen injection). The following antibodies were used: Rabbit anti-Cx43 (1:500 [58]), rat anti-ZO-1 (1:100, Millipore, Temecula, CA, USA), rabbit anti-N-Cadherin (1:500, Santa Cruz Biotechnology, CA, USA), mouse anti-N-Cadherin (1:100, BD Transduction Laboratories, San Jose, CA, USA) or rabbit anti-$Na_v1.5$ (1:100 [26]). The rabbit anti-$Na_v1.5$ antibodies were generated against an epitope of the DI–DII cytoplasmic loop specific for $Na_v1.5$. Further details can be found in [23, 30]. Statistical evaluation of co-localization was performed as described before [8].

For immunoblot analysis, total proteins were extracted from hearts of neonatal Cx43D378stop:αMyHC-Cre and adult Cx43D378stop:αMyHC-Cre-ER(T2) (14 days after last tamoxifen injection) as well as control mice. Extraction, separation, transfer and detection of proteins are described in detail in the Online Resource 1. Antibodies used were rabbit anti-Cx43 (diluted 1:500 [58]), rat anti-ZO-1 (diluted 1:200, Millipore, Temecula, CA, USA) or rabbit anti-$Na_v1.5$ (diluted 1:200, Alomone labs, Jerusalem, Israel). Loading controls were performed with mouse anti-actin (diluted 1:500, Sigma, Munich, Germany) or mouse anti-GAPDH (diluted 1:10000, Millipore, Temecula, CA, USA) antibodies.

Quantitative Real-Time-PCR—Hearts from adult Cx43D378stop:αMyHC-Cre-ER(T2) and control littermates were shock-frozen in liquid nitrogen 12 days after last tamoxifen injection. Total RNA was extracted using Trizol reagent (Invitrogen, Darmstadt, Germany). RNA was reverse transcribed into cDNA with the SuperScript VILO cDNA Synthesis Kit (Invitrogen). Quantitative PCR was performed in triplicates using Tagman Assays and Gene Expression Master Mix (Applied Biosystems) according to manufacturer's instructions. Relative expression values were normalized to the mean of controls and expressed in %±SD. Other details are given in the Online Resource 1.

Triton X-100 fractionation assay—Stable Cx43 and Cx43D378stop-expressing HeLa cells were lysed, and fractions separated by centrifugation according to their solubility to 1 % Triton X-100, based on the on the method of Musil and Goodenough (1991). Content of Cx43 in the different fractions was assessed by conventional immunoblot (details in Online Resource 1).

Co-Immunoprecipitation of ZO-1, $Na_v1.5$, and Cx43—Co-Immunoprecipitation (Co-IP) was performed using a Co-IP kit (Pierce, Rockford, IL, USA). Thousand μg protein lysate from adult Cx43D378stop hearts were prepared as described for immunoblot analyses. For pull-down of ZO-1 or $Na_v1.5$ and their interaction partners, 10 μg of ZO-1 antibodies (rabbit anti-ZO-1, Invitrogen, Darmstadt, Germany) or $Na_v1.5$ antibodies (rabbit anti $Na_v1.5$, Alomone labs, Jerusalem, Israel) were applied. Detection of Cx43, ZO-1 and $Na_v1.5$ was performed as described for immunoblot analyses.

Results

Generation of Cx43D378stop mice

For targeted mutation of the mouse Cx43 gene via homologous recombination we used the conditional Cx43D378stop-vector shown in Online Resource 2, Suppl. Fig. 1a. Blastocyst injections of correctly recombined ES cell clones yielded germ-line transmission chimeras. Breedings with C57BL/6 mice resulted in heterozygous Cx43+/floxD378stop offspring which were used for the generation of Cx43floxD378stop mutated mice with ≥87.5 % C57BL/6 genetic background. Expression of the Cx43D378stop mutation was achieved by mating Cx43floxD378stop animals with cardiomyocyte specific Cre-recombinase expressing mice (αMyHC-Cre [1] and αMyHC-Cre-ER(T2) [55]. The different genotypes

NIH-PA Author Manuscript

NIH-PA Author Manuscript

NIH-PA Author Manuscript

were confirmed by Southern blot analyses (panel b). The cardiac-directed expression of the Cx43D378stop-IRES-eGFP mRNA was verified by Northern blot analyses (panel c) and the genotype of each mouse was assessed by conventional PCR (panel d).

High lethality and absence of major structural defects in neonatal Cx43D378stop mice

Homozygous Cx43floxD378stop mice were born in corresponding Mendelian ratios. However, in contrast to control littermates all newborn homozygous Cx43D378stop mice died on the first day after birth (Fig. 1a). Morphological analyses of neonatal Cx43D378stop hearts revealed minor thickening and irregularity of the right ventricular trabeculae with abnormal pouch formation at the subpulmonary outflow tract (Fig. 1b, right panel). Yet, in contrast to Cx43 deficient neonates the pulmonary outflow tract was still open.

Electrocardiographic recordings in fetal Cx43D378stop mice

Previous studies have reported the αMyHC-promoter to be fully active at ED 13.5 with no further increase in activity beyond this day [14]. The lack of major structural cardiac abnormalities in Cx43D378stop neonates led us to speculate that death could be associated with severe cardiac arrhythmias. We therefore performed surface-ECG recordings of homozygous Cx43D378stop:αMyHC-Cre mutated fetal mice (ED 16.5) that revealed broadened QRS complexes in comparison to control mice (Fig. 1c). Statistical analysis showed a significant threefold prolongation in QRS duration in Cx43D378stop fetuses (panel d). No significant differences in beating frequency, PQ duration or QRS amplitude were observed (Online Resource 2, Suppl. Table 1).

High lethality in adult Cx43D378stop mice

To overcome neonatal lethality, homozygous Cx43floxD378stop mice were bred with Cx43+/floxD378stop:αMyHC-Cre-ER(T2) animals. Tamoxifen-induced expression of the Cx43D378stop protein in adult (3-month-old) homozygous Cx43D378stop mice resulted in death of the entire population tested, within 16–21 days after last tamoxifen injection (Fig. 2a). In contrast, control littermates injected with sterile peanut oil without tamoxifen showed 100 % survival within the same time window and no apparent change in life expectancy.

Long-term electrocardiographic recordings in adult Cx43D378stop mice

Statistical evaluation of long-term ECG recordings with conscious adult animals (recorded until death) revealed a 2.1-fold prolongation of the QRS interval in comparison to control mice (Fig. 2b). No significant differences in heart rate or PQ duration were observed (Online Resource 2, Suppl. Table 2). Northern blot analysis with RNA isolated from hearts of Cx43D378stop mice 12 days after last tamoxifen injection verified exclusive expression of the Cx43D378stop transcript after induction by tamoxifen. Representative examples of long-term ECG traces obtained from one Cx43D378stop animal are shown in panel d–h. Normal sinus rhythm without conduction disturbances or ectopic beats was present in all animals until day 13 after last tamoxifen injection (panel d). Non-sustained episodes of monomorphic and polymorphic ventricular arrhythmias were recorded by day 15–17 (panels e–f). All Cx43D378stop mice died of sustained polymorphic ventricular tachycardia finally degenerating into ventricular fibrillation (panel g). This was preceded by signs of severe conduction disturbances with unstable prolongation of the QRS interval in all animals (first occurring on day 13–14) and first degree AV-block in one animal (panel h). None of the control mice died during the observation period of 14 days, or exhibited prolongation of QRS or arrhythmias (not shown).

NIH-PA Author Manuscript

NIH-PA Author Manuscript

NIH-PA Author Manuscript

Epicardial mapping

The high propensity to ventricular arrhythmias correlated with high heterogeneity in activation times in Cx43D378stop mice, measured by field-potential mapping in the left ventricle of Langendorff-perfused hearts. Representative isochronal epicardial activation mapping 12 days after last tamoxifen injection is presented in Fig. 3a and b. The inhomogeneity index (see "Methods") revealed a very significant heterogeneity of activation in mutant mice (5.8 ± 2.5 vs 2.1 ± 0.6, $p = 0.0045$). In addition to sinus rhythm we attempted to perform activation mapping under epicardial pacing. However, fixed-rate epicardial stimulation of the ventricle induced sustained ventricular tachycardia or ventricular fibrillation in all mutant mice during the first stimulation maneuver. Within the control group no arrhythmias were seen.

Coupling analyses of Cx43D378stop gap junction channels

To study the properties of Cx43D378stop expressing cells, we cultured fetal cardiomyocytes from control and Cx43D378stop mutated hearts (ED 16.5). Dye transfer experiments showed a similar extent of intercellular neurobiotin transfer in control (Fig. 4a, left panel) and Cx43D378stop (right panel) cardiomyocytes. Statistical analysis revealed no significant difference between the groups (panel b).

For further characterization of the biophysical properties of Cx43D378stop channels, we generated stable Cx43D378stop expressing HeLa cells and performed dual whole-cell voltage clamp analyses as well as dye transfer experiments. Consistent with the dye transfer results, all examined 27 cell pairs were coupled and exhibited high junctional conductance (g_j) values (range: 6.3–127 nS; average $g_j = 55 \pm 13$ nS). Figure 4c shows records of junctional current (I_j) in response to transjunctional voltage (V_j) in the form of repeated ramps; g_j was calculated as I_j / V_j. As shown in panel c, Cx43D378stop gap junction channels exhibited octanol-induced uncoupling. Similar uncoupling was also documented during application of other *n*-alkanols, such as hexanol, heptanol, and nonanol, as well as under an exposure to 100 % CO_2. Additional experiments were performed to assess the conductance of single Cx43D378stop gap junction channels (γ_j), measured in cell pairs exhibiting low junctional conductance or during uncoupling with either *n*-alkanols or 100 % CO_2. Panel d shows the data obtained in a cell pair exhibiting only two functional channels with conductance of ~105 pS. Overall, γ_j of HeLaCx43D378stop gap junction channels ranged from 95 to 120 pS, with a mean value of 110.5 ± 1.3 pS ($n = 129$). This average value is similar to the one previously reported for wild-type Cx43 channels (115 pS; see [5]).

Furthermore, we have carried out additional experiments to examine the dependence of Cx43D378stop gap junction channels to V_j. Our results show no significant decay in I_j during ~0.5 s in response to a V_j step of –95 mV, followed by repeated V_j ramps of small amplitude (Online Resource 2, Suppl. Fig. 2a). Moreover, the g_j–V_j plot presented in Supplemental Fig. 2b (Online Resource 2) shows that the junctional conductance across Cx43D378stop gap junction channels is even less dependent on V_j than Cx43 wild-type gap junction channels. Overall, these results strongly support the notion that the increased arrhythmogenicity observed in Cx43D378stop hearts does not result from an enhanced dynamic reduction in junctional conductance associated with the V_j gating of the channel [34].

To determine single channel permeability ($P\gamma$) for Alexa fluor-350 ($P\gamma_{,AFl\text{-}350}$), experiments were performed in HeLaCx43D378stop cell pairs (Suppl. Video, Online Resource 3). We found that on average $P\gamma_{,AFl\text{-}350} = 68 \pm 12 \times 10^{-15}$ cm^3/s ($n = 6$). This value is close to the one for Cx43 gap junction channels [45]. In a similar series of experiments, we found that the permeability to the positively charged dye, (2-(4-nitro-2,1,3-

NIH-PA Author Manuscript

NIH-PA Author Manuscript

NIH-PA Author Manuscript

benzoxadiazol-7-yl)aminoethyl)trimethylammonium (EAM^+), $P\gamma_{,EAM\text{-}1}$ was $39 \pm 9 \times 10^{-15}$ cm^3/s ($n = 6$). This value is in fact higher than that reported for Cx43 gap junction channels tested with NBD-TMA^+, which is an analog of EAM-1^+ [27]. Thus, Cx43D378stop gap junction channels are permeable to positively and negatively charged dyes with single channel permeabilities similar to those of Cx43.

Cellular electrophysiology in isolated adult Cx43D378stop myocytes

The highly arrhythmogenic phenotype observed in the Cx43D378stop mice contrasted with the lack of significant changes in cell–cell coupling. We therefore explored the properties of other ion currents. Whole-cell patch clamp experiments revealed that the average peak sodium current (I_{Na}) density in Cx43D378stop cardiomyocytes was significantly reduced when compared to controls (Fig. 5a). We observed no difference in voltage-dependence of inactivation (panel b) or in the time course of recovery from inactivation (panel c) of I_{Na}, but we detected a prolongation of the time course of I_{Na} inactivation, deduced from the current elicited by a voltage pulse to –40 mV (panel d). The TTX-sensitive late sodium current was similar between mutant and control cells (Online Resource 2, Suppl. Fig. 3). Of note, ventricular myocytes from wild-type mice treated with tamoxifen displayed I_{Na} amplitude, gating and kinetics similar to those of control, showing that tamoxifen itself had no effect on I_{Na} properties (Online Resource 2, Suppl. Fig. 4).

Furthermore, we characterized the depolarization-activated outward potassium currents, and the inward rectifier current (I_{K1}) in control and Cx43D378stop adult mouse ventricular myocytes. The average peak outward current density measured at +40 mV was lower in Cx43D378stop cardiomyocytes compared to control (Fig. 5e). The magnitude and time course of current decay was best described by the sum of two exponentials, reflecting the fast ($I_{to,f}$) and slow components of inactivation ($I_{K,slow}$), plus a non-inactivating current (I_{ss}). Comparison of the individual parameters revealed a reduction in the amplitude of I_{to} when compared to control (panel f). Other parameters remained unaffected by the mutation (see also Online Resource 2, Suppl. Table 3). The density of the inward rectifier current (I_{K1}) was also not different from control (Online Resource 2, Suppl. Fig. 5).

The reduction in outward current was consistent with an increase in action potential duration at 50 and 70 % of repolarization, recorded from Cx43D378stop cardiomyocytes (Online Resource 2, Suppl. Table 4). No differences were observed in resting potential (RP), action potential amplitude (APA) or action potential duration at 90 % repolarization between the two groups (Online Resource 2, Suppl. Table 4).

Subcellular (co-)localization of intercalated disc proteins in Cx43D378stop hearts

To investigate whether localization of the alpha subunit of the cardiac sodium channel $Na_v1.5$ was affected by the Cx43D378stop mutation, we performed immunofluorescence analyses. As shown in Fig. 6a, $Na_v1.5$ preferentially localized to the area of the intercalated disc both in control and in Cx43D378stop adult hearts. Yet, the extent of $Na_v1.5$ co-localization with the adherens junctional protein N-Cadherin (as an intercalated disc marker) decreased by 34 % in Cx43D378stop hearts when compared to control (panel b). Of note, $Na_v1.5$ abundance, assessed by Immunoblot and quantitative Real-Time-PCR, was not different from control (Fig. 7f and Online Resource 2, Suppl. Fig. 6).

Furthermore, we determined the abundance and localization of Cx43 and ZO-1. Both proteins localized at end-to-end contact sites of ventricular cardiomyocytes in control (Fig. 7a) and Cx43D378stop (panel b) hearts. Statistical evaluation of the extent of co-localization revealed no significant difference between Cx43D378stop and control hearts (panel c). Moreover, Triton X-100 extraction of stably expressing HeLa cells demonstrated

NIH-PA Author Manuscript

NIH-PA Author Manuscript

NIH-PA Author Manuscript

Cx43D378stop protein expression in non-junctional (Triton X-100 soluble) and junctional (Triton X-100 insoluble) fractions (Online Resource 2, Suppl. Fig. 7). This strongly supports the notion that the Cx43D378stop protein is present in molecular aggregates, such as connexons and gap junction plaques.

Immunoblot analyses showed no significant difference in Cx43 protein levels in neonatal (Fig. 7d) and adult (Fig. 7e) Cx43D378stop hearts compared to controls. No changes in the abundance of $Na_v1.5$ or ZO-1 proteins in neonatal (panel f) or adult (panel g) Cx43D378stop hearts were detected (Online Resource 2, Suppl. Fig. 8). The distribution of actin filaments, which are connected directly to ZO-1 [25], was also unaffected by the Cx43D378stop mutation (Online Resource 2, Suppl. Fig. 9). Furthermore, Cx43D378stop, ZO-1 and $Na_v1.5$ were found in the same co-precipitate (Online Resource 2, Suppl. Fig. 10).

Discussion

Our data show that cardiac-restricted truncation of Cx43 at amino acid 378 leads to death in both neonatal and adult mice. Since ubiquitous Cx43 deficient (Cx43KO) mice die neonatally due to a malformation of the pulmonary outflow tract [46], we first investigated the cardiac morphology of neonatal Cx43D378stop hearts. We observed a minor irregular thickening of the ventricular trabeculae with an abnormal “pouch” formation at the subpulmonary outflow tract. However, in contrast to Cx43KO mice, the right ventricular outflow tract remained open. Furthermore, expression of the Cx43D378stop mutation in adult mice leads to cardiac death without any morphological abnormalities. The latter indicates that the arrhythmic phenotype of Cx43D378stop mice is independent of structural malformations.

Surface-ECG recordings of fetal Cx43D378stop mice (ED 16.5) revealed significant widening of the QRS complexes, indicating delayed ventricular conduction. This is very similar to measurements of prenatal Cx43KO mice [56]. ECG telemetry of adult conscious animals documented severe ventricular arrhythmias, ventricular fibrillation and sudden death. This phenotype is reminiscent of the one observed in adult mice with cardiac-directed knockout of Cx43. Yet, as opposed to what was observed after loss of Cx43 expression, gap junction plaques remained present at the intercalated disc in Cx43D378stop adult mice. Furthermore, functional studies showed dye transfer between myocytes isolated from these animals (Fig. 4a, b), and electrical coupling between HeLa cells expressing Cx43D378stop, with no apparent change in single-channel conductance or permeability to positively and negatively charged dyes (Fig. 4c–e). Overall, we conclude that ablation of amino acid residues 378–382 in Cx43 is sufficient to induce severe cardiac arrhythmias and death but does not prevent formation of functional Cx43 gap junction channels. Epicardial mapping showed a drastic effect on electrical heterogeneity. Patch clamp results revealed decreased I_{Na} and $I_{to,f}$ amplitudes. Yet, the consequences of the D378stop mutation may not be limited to an $I_{Na}/I_{to,f}$ deficit. In fact, it is unclear whether this mutation may alter the function of mitochondrial Cx43, causing an intracellular ionic imbalance [3, 20, 57], or alter any other cell function with indirect repercussion on electrical stability. Overall, we show that (a) residues 378–382 of Cx43 are necessary for the proper function of sodium and potassium channels, and (b) gap junction channel-independent interactions of Cx43 with other ion channel complexes are essential for normal electrical synchrony in the heart. Yet, the deficit in the sodium and transient outward current may not represent the sole effect leading to an arrhythmogenic substrate in these mice. Further studies may be necessary to investigate additional possible consequences of the Cx43D378stop truncation on cardiac arrhythmogenesis.

NIH-PA Author Manuscript

NIH-PA Author Manuscript

NIH-PA Author Manuscript

The interplay between sodium channels, junctional conductance and sink properties of the tissue downstream determine the success or failure of propagation in ventricular tissue. Recent modeling studies have demonstrated the importance of sodium channel subcellular distribution on this process (see. e.g. [31]). This distribution becomes more relevant given that the biophysical properties of channels at the intercalated disc are different from those in the midsection of the cell [35], leading investigators to conclude that the sodium channels at the intercalated disc bear the burden of excitation in the normal cardiac syncytium [35]. Additional studies show that Cx43 expression is necessary to preserve sodium current amplitude, further emphasizing the importance of proper Cx43–$Na_v1.5$ association on arrhythmogenesis [26].

Region 378–382 has been associated with the binding of Cx43 to its scaffolding protein ZO-1 [19, 24, 54]. At the resolution of confocal microscopy, however, we found Cx43 and ZO-1 still normally co-localizing to the intercalated disc of Cx43D378stop adult hearts (Fig. 7b, c). Abundance of Cx43D378stop protein was not significantly different in neonatal and adult hearts compared to controls (Fig. 7d, e). Cx43 and ZO-1 were also found in the same immune precipitate (Online Resource 2, Suppl. Fig. 10). We speculate that ablation of the last five amino acid residues of Cx43 may still allow interaction(s) between Cx43 and ZO-1 via other partners or a second ZO-1 binding site, which has been suggested before [52, 54]. Overall, our results suggest that distribution of Cx43 and ZO-1 seems to be preserved following the Cx43 truncation. On the other hand, our results do not discard the possibility that deletion of residues 378–382 alters the binding state of Cx43 to ZO-1, which could play a role in the generation of cardiac arrhythmias detected in the Cx43D378stop mice. In that regard, it is important to note previous studies suggesting that the area surrounding a gap junction plaque is populated by Cx43 connexons that associate with ZO-1 and that are not involved in forming gap junctions. This region, dubbed “the perinexus” [47], emerges as a likely candidate for the site of interactions between Cx43 and other molecules (such as the sodium channel complex [10, 12, 48]). Furthermore, the same group reported an increase in gap junction plaque size when interrupting Cx43/ZO-1 interaction [24, 47]. Yet, in our Cx43D378stop mouse model we did not find larger gap junction plaques at the intercalated discs relative to controls by confocal microscopy. However, in their studies, Rhett et al. [47] utilized the Duolink method to define the perinexus in cultured cells. Further technical development remains necessary to make the Duolink methodology applicable to cardiac tissue, so that the structure of the perinexus, in the context of the cardiac intercalated disc, can be defined.

Besides gap junction channels, ion channel complexes are important for electrical function of the heart. Our studies revealed a significant decrease in the peak average I_{Na} density, as well as decreased abundance of $Na_v1.5$ co-localizing with N-Cadherin in Cx43D378stop hearts (Figs. 5, 6). Since total expression levels of $Na_v1.5$ were not changed in Cx43D378stop hearts (Fig. 7g), we assume $Na_v1.5$ molecules to be dispersed inside the cell of Cx43D378stop hearts, and therefore, not detectable by confocal microscopy. A similar effect has been reported before for other proteins that cluster in plaque structures [28]. Cardiac-directed loss of Cx43 in the heart (Cx43KO) has been shown to be accompanied by reduced I_{Na} and $Na_v1.5$ at the intercalated disc [13]. The question arises as to whether the phenotype of the Cx43D378stop simply reflects the absence of an important functional region, or whether the truncated protein has a harmful effect on ion channels, beyond what is consequent to the simple absence of region 378–382. The latter seems the more likely scenario. First, in addition to the loss of I_{Na} density, we observed a prolongation of the time course of I_{Na} inactivation in D378stop animals, which does not occur in cells from Cx43KO mice ([26] and unpublished observations from our lab). Second, the effects observed in outward currents are opposite to those reported for Cx43-KO mice [9]. Third, the high incidence of death in Cx43D378stop mice contrasts with the higher survival observed in

NIH-PA Author Manuscript

NIH-PA Author Manuscript

NIH-PA Author Manuscript

mice expressing the Cx43K258stop mutation where the last 125 amino acid residues are missing ([37]; however, see also other aspects below). Altogether, we speculate that the Cx43D378stop protein negatively influences cardiac electrical behavior beyond what is expected from the absence of the 378–382 regions.

Seen from a different angle, we speculate that the region 378–382 of Cx43 has a protective effect on cardiac electrophysiology. This is consistent with results showing that a peptide matching the C-terminal sequence of Cx43 ("αCT-1") prevents arrhythmias [41]. In addition to its effect as a competitive inhibitor of Cx43-ZO-1 binding [24] αCT-1 may directly protect the function of other ion channels because of its similarity with the Cx43 C-terminal (CT) sequence. The "anti-arrhythmic" role of region 378–382 may involve masking a separate region of the Cx43CT that, if unmasked, exerts a negative effect on other ion channels. This idea is consistent with previous observations showing extensive intramolecular interactions in the Cx43 protein [22, 29]. The idea is also consistent with the observation that mice with a larger truncation of Cx43 (K258stop [36, 38]) do not exhibit spontaneous lethal arrhythmias. Comparisons of D378stop vs K258stop mice, however, should be made with caution. Indeed, to overcome perinatal death, K258stop animals were crossed with Cx43KO mice, and studies were conducted in heterozygous K258stop/KO mice. In contrast, D378stop mice are homozygous. Also of note, K258stop expression was constitutive, rather than tamoxifen induced as in Cx43D378stop mice. Whether there are adaptive processes in K258stop/KO animals during development that protect from arrhythmias remains to be determined.

It has been reported before that Cx43 can be co-immuno-precipitated with $Na_v1.5$ antibodies [39], however, the molecular mechanisms linking Cx43 expression and/or structural integrity to the sodium channel complex remain undefined. Moreover, we also show the presence of Cx43D378stop and $Na_v1.5$ in the same immuno-precipitate (Online Resource 2, Suppl. Fig. 10). We speculate that these interactions are indirect and perhaps involve changes in the trafficking of $Na_v1.5$ to its location at the intercalated disc. Indeed, while previous studies indicate that the microtubular network is necessary for Cx43 trafficking and gap junction assembly [53], recent work shows that Cx43 is, in turn, a regulator of microtubular dynamics [16, 17]. We speculate that proteins trafficking the microtubular network fail to reach the membrane if Cx43 is not properly expressed or localized. Based on a recent study showing that $Na_v1.5$ traffics through the microtubular network [6], we propose that Cx43-mediated microtubular stabilization is required for the trafficking of $Na_v1.5$ to the intercalated disc. It remains to be investigated whether a similar process regulates the assembly of the molecular complex responsible for the I_{to} current.

Our data show that the presence and function of Cx43D378stop gap junction channels are similar to wild-type Cx43 channels. Overall, our data suggest that the Cx43D378stop arrhythmic phenotype is not consequent to loss of gap junction-mediated conductance. Instead, we conclude that deletion of the last five amino acid residues of the Cx43 C-terminus leads to coupling-unrelated modifications sufficient to induce cardiac arrhythmias and death. As such, Cx43 emerges not only as the key constitutive molecule of gap junctions, but also as a critical regulator of excitability and repolarization. Cell excitability and cell–cell propagation of electrical signals may be the two functions of one common supramolecular complex at the cardiac intercalated disc. Our results suggest that the function of this supramolecular complex should be taken into account when cardiac diseases affecting impulse conduction and excitability are to be mechanistically explained. New therapeutic drugs for these diseases may not only affect the target protein against which they were developed, but also the components of this complex.

NIH-PA Author Manuscript

NIH-PA Author Manuscript

NIH-PA Author Manuscript

Supplementary Material

Refer to Web version on PubMed Central for supplementary material.

Acknowledgments

This work was supported by Grants of the German Research Foundation [Wi270/32-1 and SFB 645, B2 to K.W.; FL 276/3-3 to B.K.F. and P.S.], the National Institutes of Health [R01 HL106632-01, R01 GM57691-13 to M.D.; R01NS072238, RO1HL084464 to F.F.B., as well as NIH HL084583, HL083422 to P J M], the Leducq Foundation to M.D., as well as the American Heart Association and the Saving Tiny Hearts Society to P.J.M.I.L. gratefully acknowledges a PhD stipend of the Jürgen-Manchot-Foundation. We thank Melanie Jokwitz and Christine Siegmund for excellent technical assistance and blastocyst injections.

References

1. Agah R, Frenkel PA, French BA, Michael LH, Overbeek PA, Schneider MD. Gene recombination in postmitotic cells. Targeted expression of Cre recombinase provokes cardiac-restricted, site-specific rearrangement in adult ventricular muscle in vivo. J Clin Invest. 1997; 100:169–179. doi: 10.1172/JCI119509. [PubMed: 9202069]
2. Asimaki A, Tandri H, Huang H, Halushka MK, Gautam S, Basso C, Thiene G, Tsatsopoulou A, Protonotarios N, McKenna WJ, Calkins H, Saffitz JE. A new diagnostic test for arrhythmogenic right ventricular cardiomyopathy. N Engl J Med. 2009; 360:1075–1084. doi:10.1056/NEJMoa0808138. [PubMed: 19279339]
3. Boengler K, Dodoni G, Rodriguez-Sinovas A, Cabestrero A, Ruiz-Meana M, Gres P, Konietzka I, Lopez-Iglesias C, Garcia-Dorado D, Di Lisa F, Heusch G, Schulz R. Connexin 43 in cardiomyocyte mitochondria and its increase by ischemic preconditioning. Cardiovasc Res. 2005; 67:234–244. doi: 10.1016/j.cardiores.2005.04.014. [PubMed: 15919068]
4. Bruce AF, Rothery S, Dupont E, Severs NJ. Gap junction remodelling in human heart failure is associated with increased interaction of connexin 43 with ZO-1. Cardiovasc Res. 2008; 77:757–765. doi:10.1093/cvr/cvm083. [PubMed: 18056766]
5. Bukauskas FF, Verselis VK. Gap junction channel gating. Biochim Biophys Acta. 2004; 1662:42–60. doi:10.1016/j.bbamem.2004.01.008. [PubMed: 15033578]
6. Casini S, Tan HL, Demirayak I, Remme CA, Amin AS, Scicluna BP, Chatyan H, Ruijter JM, Bezzina CR, van Ginneken AC, Veldkamp MW. Tubulin polymerization modifies cardiac sodium channel expression and gating. Cardiovasc Res. 2010; 85:691–700. doi:10.1093/cvr/cvp352. [PubMed: 19861310]
7. Cheng L, Yung A, Covarrubias M, Radice GL. Cortactin is required for N-cadherin regulation of Kv 1.5 channel function. J Biol Chem. 2011; 286:20478–20489. doi:10.1074/jbc.M111.218560. [PubMed: 21507952]
8. Chkourko HS, Guerrero-Serna G, Lin X, Darwish N, Pohlmann JR, Cook KE, Martens JR, Rothenberg E, Musa H, Delmar M. Remodeling of mechanical junctions and of microtubule-associated proteins accompany cardiac connexin43 lateralization. Heart Rhythm. 2012; 9(1133–1140):e1136. doi:10.1016/j.hrthm.2012.03.003.
9. Danik SB, Rosner G, Lader J, Gutstein DE, Fishman GI, Morley GE. Electrical remodeling contributes to complex tachyarrhythmias in connexin43-deficient mouse hearts. FASEB J. 2008; 22:1204–1212. doi:10.1096/fj.07-8974com. [PubMed: 17984180]
10. Delmar M. Connexin43 regulates sodium current; ankyrin-G modulates gap junctions: the intercalated disc exchanger. Cardiovasc Res. 2012; 93:220–222. doi:10.1093/cvr/cvr343. [PubMed: 22180603]
11. Delmar M. Desmosome-ion channel interactions and their possible role in arrhythmogenic cardiomyopathy. Pediatr Cardiol. 2012; 33:975–979. doi:10.1007/s00246-012-0257-0. [PubMed: 22407454]
12. Delmar M, Liang FX. Connexin43 and the regulation of intercalated disc function. Heart Rhythm. 2012; 9:835–838. doi: 10.1016/j.hrthm.2011.10.028. [PubMed: 22056332]
13. Desplantez T, McCain ML, Beauchamp P, Rigoli G, Rothen-Rutishauser B, Parker KK, Kleber AG. Connexin43 ablation in foetal atrial myocytes decreases electrical coupling, partner

NIH-PA Author Manuscript

NIH-PA Author Manuscript

NIH-PA Author Manuscript

connexins, and sodium current. Cardiovasc Res. 2012; 94:58–65. doi:10.1093/cvr/cvs025. [PubMed: 22287588]

14. Eckardt D, Kirchhoff S, Kim JS, Degen J, Theis M, Ott T, Wiesmann F, Doevendans PA, Lamers WH, de Bakker JM, van Rijen HV, Schneider MD, Willecke K. Cardiomyocyte-restricted deletion of connexin43 during mouse development. J Mol Cell Cardiol. 2006; 41:963–971. doi:10.1016/j.yjmcc.2006.07.017. [PubMed: 16963078]
15. Eckardt D, Theis M, Degen J, Ott T, van Rijen HV, Kirchhoff S, Kim JS, de Bakker JM, Willecke K. Functional role of connexin43 gap junction channels in adult mouse heart assessed by inducible gene deletion. J Mol Cell Cardiol. 2004; 36:101–110. [PubMed: 14734052]
16. Fontes MS, van Veen TA, de Bakker JM, van Rijen HV. Functional consequences of abnormal Cx43 expression in the heart. Biochim Biophys Acta. 2012; 1818:2020–2029. doi:10.1016/j.bbamem.2011.07.039. [PubMed: 21839722]
17. Francis R, Xu X, Park H, Wei CJ, Chang S, Chatterjee B, Lo C. Connexin43 modulates cell polarity and directional cell migration by regulating microtubule dynamics. PLoS ONE. 2011; 6:e26379. doi:10.1371/journal.pone.0026379. [PubMed: 22022608]
18. Franke WW, Schumacher H, Borrmann CM, Grund C, Winter-Simanowski S, Schlechter T, Pieperhoff S, Hofmann I. The area composita of adhering junctions connecting heart muscle cells of vertebrates-III: assembly and disintegration of intercalated disks in rat cardiomyocytes growing in culture. Eur J Cell Biol. 2007; 86:127–142. doi:10.1016/j.ejcb.2006.11.003. [PubMed: 17275137]
19. Giepmans BN, Moolenaar WH. The gap junction protein connexin43 interacts with the second PDZ domain of the zona occludens-1 protein. Curr Biol. 1998; 8:931–934. [PubMed: 9707407]
20. Heinzel FR, Luo Y, Li X, Boengler K, Buechert A, Garcia-Dorado D, Di Lisa F, Schulz R, Heusch G. Impairment of diazoxide-induced formation of reactive oxygen species and loss of cardioprotection in connexin 43 deficient mice. Circ Res. 2005; 97:583–586. doi:10.1161/01.RES.0000181171.65293.65. [PubMed: 16100048]
21. Herr C, Smyth N, Ullrich S, Yun F, Sasse P, Hescheler J, Fleischmann B, Lasek K, Brixius K, Schwinger RH, Fassler R, Schroder R, Noegel AA. Loss of annexin A7 leads to alterations in frequency-induced shortening of isolated murine cardiomyocytes. Mol Cell Biol. 2001; 21:4119–4128. doi:10.1128/MCB.21.13.4119-4128.2001. [PubMed: 11390641]
22. Hirst-Jensen BJ, Sahoo P, Kieken F, Delmar M, Sorgen PL. Characterization of the pH-dependent interaction between the gap junction protein connexin43 carboxyl terminus and cytoplasmic loop domains. J Biol Chem. 2007; 282:5801–5813. doi:10.1074/jbc.M605233200. [PubMed: 17178730]
23. Hund TJ, Koval OM, Li J, Wright PJ, Qian L, Snyder JS, Gudmundsson H, Kline CF, Davidson NP, Cardona N, Rasband MN, Anderson ME, Mohler PJ. A beta(IV)-spectrin/CaMKII signaling complex is essential for membrane excitability in mice. J Clin Invest. 2010; 120:3508–3519. doi:10.1172/JCI43621. [PubMed: 20877009]
24. Hunter AW, Barker RJ, Zhu C, Gourdie RG. Zonula occludens-1 alters connexin43 gap junction size and organization by influencing channel accretion. Mol Biol Cell. 2005; 16:5686–5698. doi:10.1091/mbc.E05-08-0737. [PubMed: 16195341]
25. Itoh M, Nagafuchi A, Moroi S, Tsukita S. Involvement of ZO-1 in cadherin-based cell adhesion through its direct binding to alpha catenin and actin filaments. J Cell Biol. 1997; 138:181–192. [PubMed: 9214391]
26. Jansen JA, Noorman M, Musa H, Stein M, de Jong S, van der Nagel R, Hund TJ, Mohler PJ, Vos MA, van Veen TA, de Bakker JM, Delmar M, van Rijen HV. Reduced heterogeneous expression of Cx43 results in decreased $Na_v1.5$ expression and reduced sodium current that accounts for arrhythmia vulnerability in conditional Cx43 knockout mice. Heart Rhythm. 2012; 9:600–607. doi:10.1016/j.hrthm.2011.11.025. [PubMed: 22100711]
27. Kanaporis G, Brink PR, Valiunas V. Gap junction permeability: selectivity for anionic and cationic probes. Am J Physiol Cell Physiol. 2011; 300:C600–C609. doi:10.1152/ajpcell.00316.2010. [PubMed: 21148413]
28. Kaplan SR, Gard JJ, Protonotarios N, Tsatsopoulou A, Spiliopoulou C, Anastasakis A, Squarcioni CP, McKenna WJ, Thiene G, Basso C, Brousse N, Fontaine G, Saffitz JE. Remodeling of myocyte gap junctions in arrhythmogenic right ventricular cardiomyopathy due to a deletion in plakoglobin

NIH-PA Author Manuscript

NIH-PA Author Manuscript

NIH-PA Author Manuscript

(Naxos disease). Heart Rhythm. 2004; 1:3–11. doi:10.1016/j.hrthm.2004.01.001. [PubMed: 15851108]

29. Kieken F, Mutsaers N, Dolmatova E, Virgil K, Wit AL, Kellezi A, Hirst-Jensen BJ, Duffy HS, Sorgen PL. Structural and molecular mechanisms of gap junction remodeling in epicardial border zone myocytes following myocardial infarction. Circ Res. 2009; 104:1103–1112. doi:10.1161/CIRCRESAHA.108.190454. [PubMed: 19342602]
30. Koval OM, Snyder JS, Wolf RM, Pavlovicz RE, Glynn P, Curran J, Leymaster ND, Dun W, Wright PJ, Cardona N, Qian L, Mitchell CC, Boyden PA, Binkley PF, Li C, Anderson ME, Mohler PJ, Hund TJ. Ca^{2+}/calmodulin-dependent protein kinase II-based regulation of voltage-gated Na^{+} channel in cardiac disease. Circulation. 2012; 126:2084–2094. doi:10.1161/CIRCULATIONAHA.112.105320. [PubMed: 23008441]
31. Kucera JP, Rohr S, Rudy Y. Localization of sodium channels in intercalated disks modulates cardiac conduction. Circ Res. 2002; 91:1176–1182. [PubMed: 12480819]
32. Lammers WJ, Schalij MJ, Kirchhof CJ, Allessie MA. Quantification of spatial inhomogeneity in conduction and initiation of reentrant atrial arrhythmias. Am J Physiol. 1990; 259:H1254–H1263. [PubMed: 1699438]
33. Li J, Goossens S, van Hengel J, Gao E, Cheng L, Tyberghein K, Shang X, De Rycke R, van Roy F, Radice GL. Loss of alphaT-catenin alters the hybrid adhering junctions in the heart and leads to dilated cardiomyopathy and ventricular arrhythmia following acute ischemia. J Cell Sci. 2012; 125:1058–1067. doi: 10.1242/jcs.098640. [PubMed: 22421363]
34. Lin X, Gemel J, Beyer EC, Veenstra RD. Dynamic model for ventricular junctional conductance during the cardiac action potential. Am J Physiol Heart Circ Physiol. 2005; 288:H1113–H1123. doi:10.1152/ajpheart.00882.2004. [PubMed: 15513960]
35. Lin X, Liu N, Lu J, Zhang J, Anumonwo JM, Isom LL, Fishman GI, Delmar M. Subcellular heterogeneity of sodium current properties in adult cardiac ventricular myocytes. Heart Rhythm. 2011; 8:1923–1930. doi:10.1016/j.hrthm.2011.07.016. [PubMed: 21767519]
36. Maass K, Chase SE, Lin X, Delmar M. Cx43 CT domain influences infarct size and susceptibility to ventricular tachyarrhythmias in acute myocardial infarction. Cardiovasc Res. 2009; 84:361–367. doi:10.1093/cvr/cvp250. [PubMed: 19620131]
37. Maass K, Ghanem A, Kim JS, Saathoff M, Urschel S, Kirfel G, Grummer R, Kretz M, Lewalter T, Tiemann K, Winterhager E, Herzog V, Willecke K. Defective epidermal barrier in neonatal mice lacking the C-terminal region of connexin43. Mol Biol Cell. 2004; 15:4597–4608. doi:10.1091/mbc.E04-04-0324. [PubMed: 15282340]
38. Maass K, Shibayama J, Chase SE, Willecke K, Delmar M. C-terminal truncation of connexin43 changes number, size, and localization of cardiac gap junction plaques. Circ Res. 2007; 101:1283–1291. doi:10.1161/CIRCRESAHA.107.162818. [PubMed: 17932323]
39. Malhotra JD, Thyagarajan V, Chen C, Isom LL. Tyrosinephosphorylated and nonphosphorylated sodium channel beta1 subunits are differentially localized in cardiac myocytes. J Biol Chem. 2004; 279:40748–40754. doi:10.1074/jbc.M407243200. [PubMed: 15272007]
40. Murray KT, Anno T, Bennett PB, Hondeghem LM. Voltage clamp of the cardiac sodium current at 37 °C in physiologic solutions. Biophys J. 1990; 57:607–613. doi:10.1016/S0006-3495(90)82576-5. [PubMed: 2155034]
41. O'Quinn MP, Palatinus JA, Harris BS, Hewett KW, Gourdie RG. A peptide mimetic of the connexin43 carboxyl terminus reduces gap junction remodeling and induced arrhythmia following ventricular injury. Circ Res. 2011; 108:704–715. doi: 10.1161/CIRCRESAHA.110.235747. [PubMed: 21273554]
42. Peters NS, Green CR, Poole-Wilson PA, Severs NJ. Reduced content of connexin43 gap junctions in ventricular myocardium from hypertrophied and ischemic human hearts. Circulation. 1993; 88:864–875. [PubMed: 8394786]
43. Petitprez S, Zmoos AF, Ogrodnik J, Balse E, Raad N, El-Haou S, Albesa M, Bittihn P, Luther S, Lehnart SE, Hatem SN, Coulombe A, Abriel H. SAP97 and dystrophin macromolecular complexes determine two pools of cardiac sodium channels $Na_V1.5$ in cardiomyocytes. Circ Res. 2011; 108:294–304. doi:10.1161/CIRCRESAHA.110.228312. [PubMed: 21164104]

NIH-PA Author Manuscript

NIH-PA Author Manuscript

NIH-PA Author Manuscript

44. Rackauskas M, Kreuzberg MM, Pranevicius M, Willecke K, Verselis VK, Bukauskas FF. Gating properties of heterotypic gap junction channels formed of connexins 40, 43, and 45. Biophys J. 2007; 92:1952–1965. doi:10.1529/biophysj.106.099358. [PubMed: 17189315]
45. Rackauskas M, Verselis VK, Bukauskas FF. Permeability of homotypic and heterotypic gap junction channels formed of cardiac connexins mCx30.2, Cx40, Cx43, and Cx45. Am J Physiol Heart Circ Physiol. 2007; 293:H1729–H1736. doi: 10.1152/ajpheart.00234.2007. [PubMed: 17557922]
46. Reaume AG, de Sousa PA, Kulkarni S, Langille BL, Zhu D, Davies TC, Juneja SC, Kidder GM, Rossant J. Cardiac malformation in neonatal mice lacking connexin43. Science. 1995; 267:1831–1834. [PubMed: 7892609]
47. Rhett JM, Jourdan J, Gourdie RG. Connexin 43 connexon to gap junction transition is regulated by zonula occludens-1. Mol Biol Cell. 2011; 22:1516–1528. doi:10.1091/mbc.E10-06-0548. [PubMed: 21411628]
48. Rhett JM, Ongstad EL, Jourdan J, Gourdie RG. Cx43 associates with Na(v)1.5 in the cardiomyocyte perinexus. J Membr Biol. 2012; 245:411–422. doi:10.1007/s00232-012-9465-z. [PubMed: 22811280]
49. Sato PY, Coombs W, Lin X, Nekrasova O, Green KJ, Isom LL, Taffet SM, Delmar M. Interactions between ankyrin-G, plakophilin-2, and connexin43 at the cardiac intercalated disc. Circ Res. 2011; 109:193–201. doi:10.1161/CIRCRESAHA.111.247023. [PubMed: 21617128]
50. Sato PY, Musa H, Coombs W, Guerrero-Serna G, Patino GA, Taffet SM, Isom LL, Delmar M. Loss of plakophilin-2 expression leads to decreased sodium current and slower conduction velocity in cultured cardiac myocytes. Circ Res. 2009; 105:523–526. doi:10.1161/CIRCRESAHA.109.201418. [PubMed: 19661460]
51. Schrickel JW, Brixius K, Herr C, Clemen CS, Sasse P, Reetz K, Grohe C, Meyer R, Tiemann K, Schroder R, Bloch W, Nickenig G, Fleischmann BK, Noegel AA, Schwinger RH, Lewalter T. Enhanced heterogeneity of myocardial conduction and severe cardiac electrical instability in annexin A7-deficient mice. Cardiovasc Res. 2007; 76:257–268. doi:10.1016/j.cardiores.2007.07.001. [PubMed: 17662970]
52. Severs NJ. The carboxy terminal domain of connexin43: from molecular regulation of the gap junction channel to supra-molecular organization of the intercalated disk. Circ Res. 2007; 101:1213–1215. doi:10.1161/CIRCRESAHA.107.165662. [PubMed: 18063815]
53. Shaw RM, Fay AJ, Puthenveedu MA, von Zastrow M, Jan YN, Jan LY. Microtubule plus-end-tracking proteins target gap junctions directly from the cell interior to adherens junctions. Cell. 2007; 128:547–560. doi:10.1016/j.cell.2006.12.037. [PubMed: 17289573]
54. Sorgen PL, Duffy HS, Sahoo P, Coombs W, Delmar M, Spray DC. Structural changes in the carboxyl terminus of the gap junction protein connexin43 indicates signaling between binding domains for c-Src and zonula occludens-1. J Biol Chem. 2004; 279:54695–54701. doi:10.1074/jbc.M409552200. [PubMed: 15492000]
55. Takefuji M, Wirth A, Lukasova M, Takefuji S, Boettger T, Braun T, Althoff T, Offermanns S, Wettschureck N. G(13)-mediated signaling pathway is required for pressure overload-induced cardiac remodeling and heart failure. Circulation. 2012; 126:1972–1982. doi:10.1161/CIRCULATIONAHA.112.109256. [PubMed: 22972902]
56. Vaidya D, Tamaddon HS, Lo CW, Taffet SM, Delmar M, Morley GE, Jalife J. Null mutation of connexin43 causes slow propagation of ventricular activation in the late stages of mouse embryonic development. Circ Res. 2001; 88:1196–1202. [PubMed: 11397787]
57. Wang N, De Vuyst E, Ponsaerts R, Boengler K, Palacios-Prado N, Wauman J, Lai CP, De Bock M, Decrock E, Bol M, Vinken M, Rogiers V, Tavernier J, Evans WH, Naus CC, Bukauskas FF, Sipido KR, Heusch G, Schulz R, Bultynck G, Leybaert L. Selective inhibition of Cx43 hemichannels by Gap19 and its impact on myocardial ischemia/reperfusion injury. Basic Res Cardiol. 2013; 108:309. doi:10.1007/s00395-012-0309-x. [PubMed: 23184389]
58. Yeager M, Gilula NB. Membrane topology and quaternary structure of cardiac gap junction ion channels. J Mol Biol. 1992; 223:929–948. [PubMed: 1371548]

NIH-PA Author Manuscript

NIH-PA Author Manuscript

NIH-PA Author Manuscript

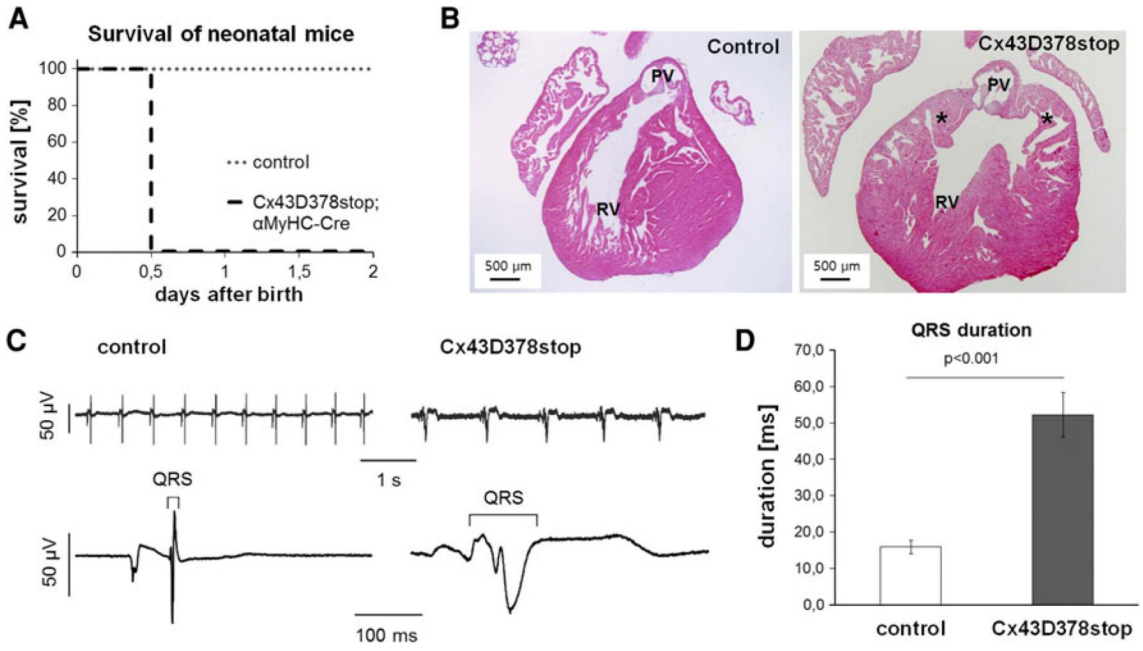

Fig. 1.

Lethality and impaired cardiac conduction in neonatal Cx43D378stop mice. **a** Homozygous Cx43D378stop:αMyHC-Cre mice die within the first day after birth. In contrast, control littermates (heterozygous Cx43D378stop, heterozygous or homozygous Cx43floxD378stop mice) showed a normal life expectancy after birth. $n > 10$ per group. **b** In contrast to controls (*left panel*) newborn Cx43D378stop hearts (*right panel*) display irregular thickened trabeculae with abnormal pouch formation (*asterisk*) at the subpulmonary outflow tract but in contrast to Cx43KO mice the pulmonary outflow tract is still open. PV, pulmonary vein; RV, right ventricle. $n > 7$ per group. **c** Representative examples of surface-ECG recordings of a control (*left*) and a Cx43D378stop (*right*) fetus (ED 16.5). **d** Statistical analysis reveal significantly 3.3-fold prolonged QRS intervals in mutant mice compared to controls. $n = 6$ for Cx43D378stop and $n = 7$ for control mice

NIH-PA Author Manuscript
NIH-PA Author Manuscript
NIH-PA Author Manuscript

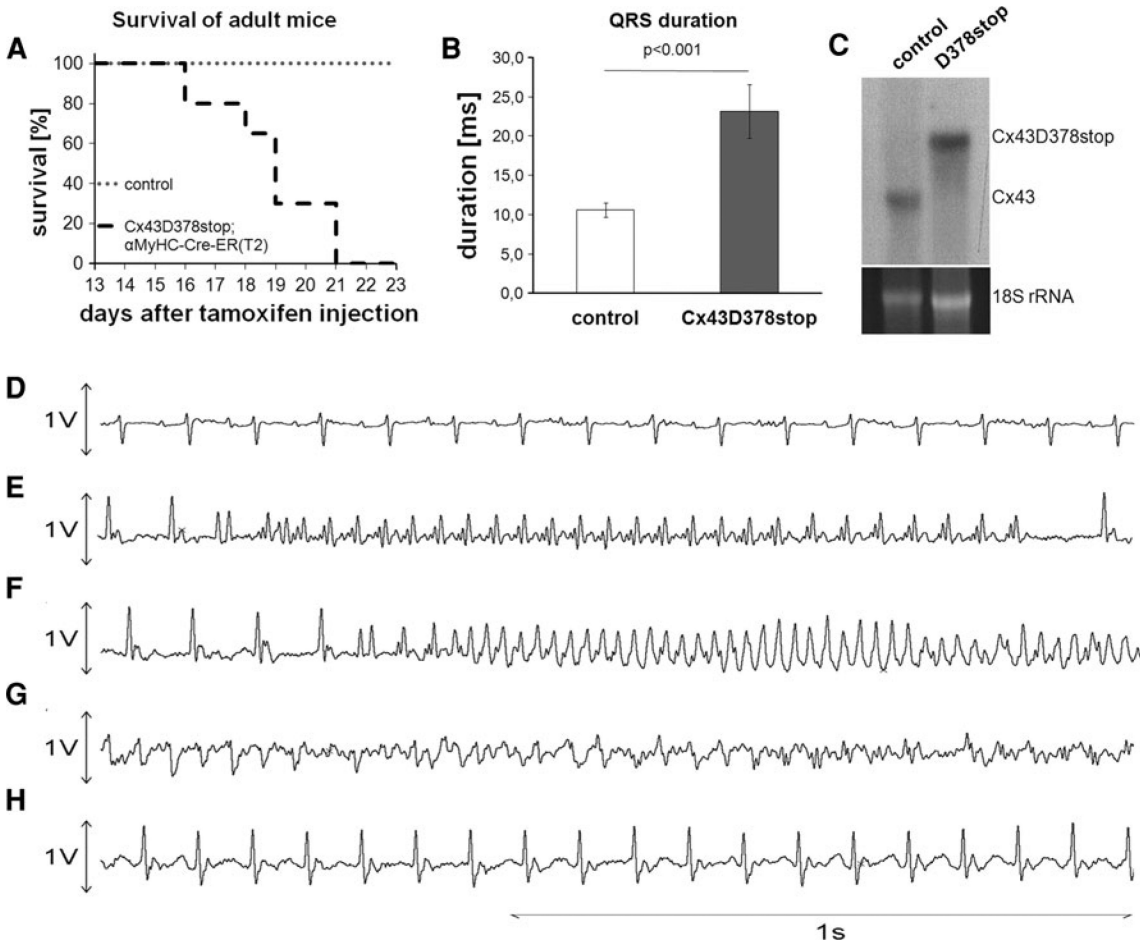

Fig. 2.

Lethal ventricular arrhythmias in adult Cx43D378stop mice. **a** Tamoxifen-injected adult (3-month-old) homozygous Cx43D378stop:αMyHC-Cre-ER(T2) mice die between day 16 and 21 after last tamoxifen injection. In contrast, oil-injected control littermates (heterozygous or homozygous Cx43floxD378stop mice) survived normally. $n > 10$ per group. **b** Statistical evaluation of the QRS interval in long-tem ECG recordings revealed a 2.1-fold prolongation of ventricular depolarization in comparison to control mice. $n = 4$ per group. **c** Northern blot analysis verified expression of the Cx43D378stop mRNA and absence of Cx43 mRNA in adult Cx43D378stop mice 12 days after last tamoxifen injection. **d–g** Representative long-term ECG recordings of a Cx43D378stop mutated mouse recorded until its death. **d** Normal sinus rhythm at the start of recording on day 10 after last tamoxifen injection. **e** First occurrence of non-sustained monomorphic tachycardia on day 15. **f** Polymorphic tachycardia on day 17. **g** Polymorphic tachycardia, degenerating in ventricular fibrillation, causing death on day 18. **h** QRS prolongation and bundle branch block deformation on day 15

NIH-PA Author Manuscript

NIH-PA Author Manuscript

NIH-PA Author Manuscript

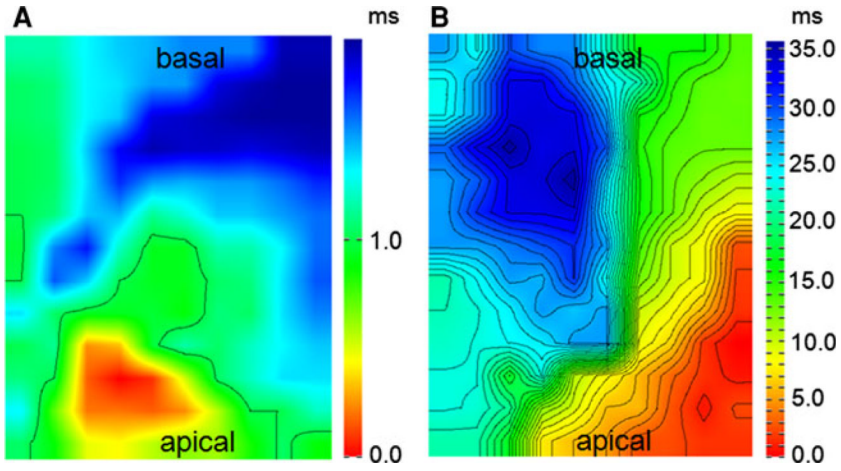

Fig. 3.

Epicardial mapping of Langendorff-perfused hearts from control and Cx43D378stop mice. Representative examples of spontaneous conduction in the left ventricle of a control animal (**a**) and a Cx43D378stop mouse (**b**) during sinus rhythm. Isochronal maps show a broad conduction delay in mutant mice. Isochronal lines are shown at distances of 1 ms. $n = 3$ per group

NIH-PA Author Manuscript

NIH-PA Author Manuscript

NIH-PA Author Manuscript

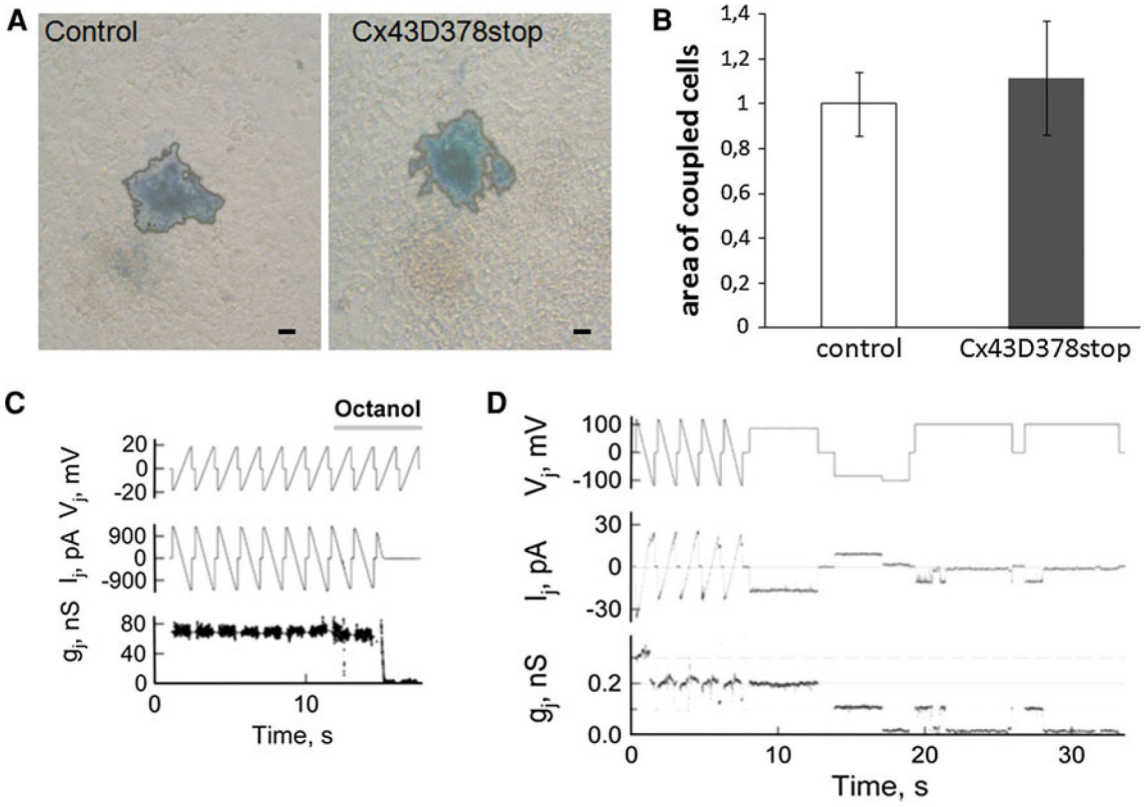

Fig. 4.

Coupling analysis of Cx43D378stop gap junction channels. Injection of neurobiotin into one cell at the periphery of beating cardiomyocyte clusters leads to intercellular dye transfer between neighboring cells in control (**a**, *left panel*) and Cx43D378stop:αMyHC-Cre (**a**, *right panel*) cardiomyocytes indicated by *blue* color. For better evaluation, the *blue* colored area was bordered by a *black line*. Statistical analysis of the coupling experiments revealed no significant difference in coupling among Cx43D378stop:αMyHC-Cre compared to control cardiomyocytes (**b**). Data are mean ± SEM of ≥20 injections in each cell line. *Bar*: 20 μm. **c** Application of octanol (2 mM) produced full uncoupling of Cx43D378stop homotypic junctions within ~3 s. Repeated ramps of voltage (V_j) were used to measure junctional current (I_j). Junctional conductance was calculated from the ratio, I_j/V_j. **d** Single channel events measured in HeLaCx43D378stop cell pair during an exposure to CO_2 that reduced cell–cell coupling initially to three and at the end of the recording to one functional channel with conductance of ~105 pS. $n = 27$ for junctional conductance and $n = 129$ for single channel events

NIH-PA Author Manuscript
NIH-PA Author Manuscript
NIH-PA Author Manuscript

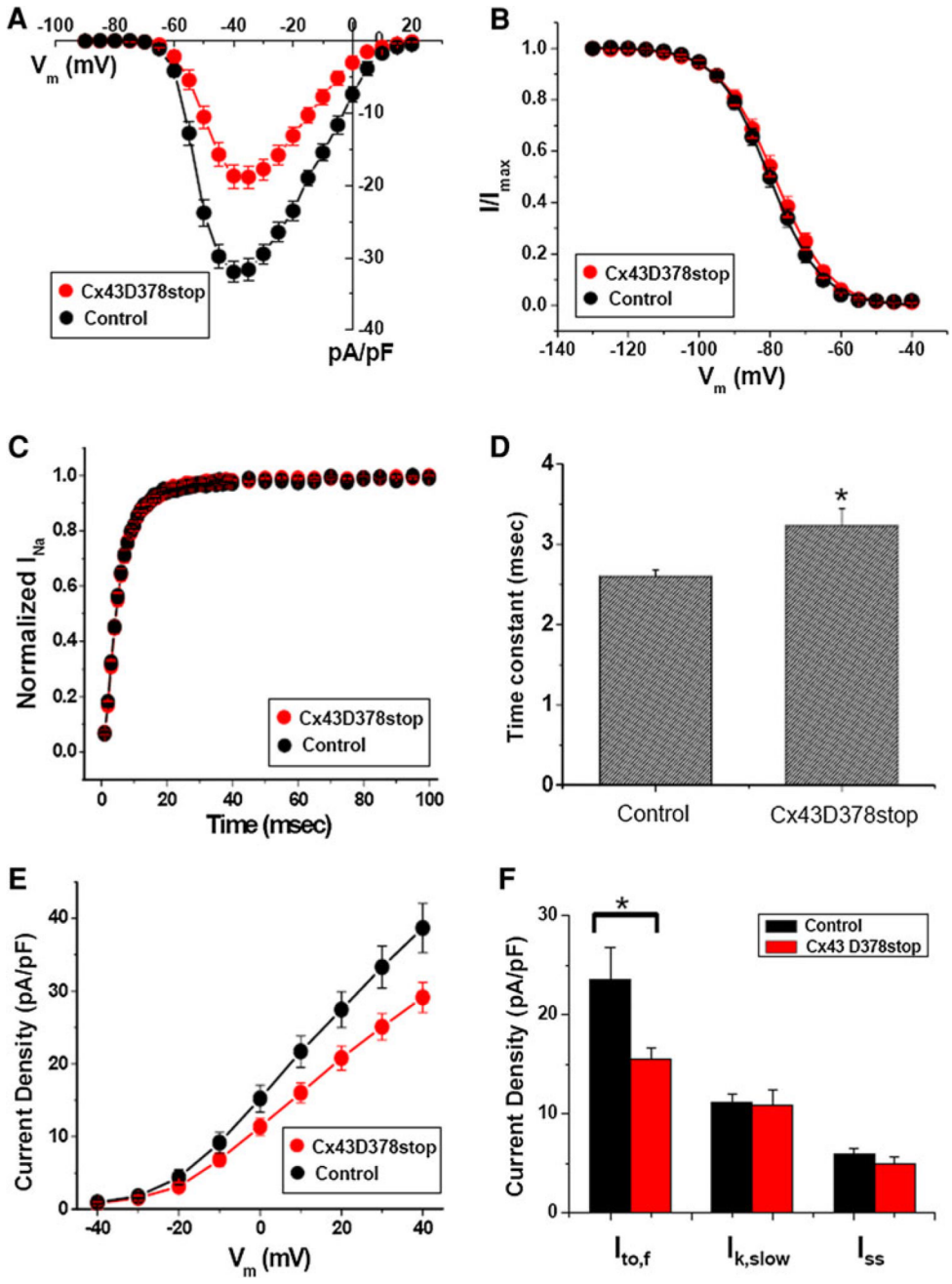

Fig. 5.

Sodium current and depolarization-activated outward potassium current properties recorded from adult cardiac myocytes isolated from Cx43D378stop hearts. **a** Average peak sodium current density as a function of voltage command. Peak current amplitude at –40 mV: Control: –32.0 ± 1.5 pA/pF; $n = 13$. Cx43D378stop: –18.7 ± 2.1 pA/pF; $n = 14$. $P < 0.001$. **b** Voltage-dependence of I_{Na} steady-state inactivation curves. Voltage for half-maximal inactivation ($V_{1/2}$):–80.2 ± 1.2 mV for control and 78.7 ± 1.4 mV for Cx43D378stop (pNS). **c** Time course of I_{Na} recovery from inactivation. Time constant (one exponential function): 5.1 ± 0.3 ms for control and 5.3 ± 0.4 ms for Cx43D378stop (pNS). **d** Inactivation time course (one exponential function) of I_{Na}: 2.6 ± 0.1 ms for control and 3.2 ± 0.2 ms for Cx43D378stop, $P < 0.04$. **e** Average peak potassium current density as a function of voltage

NIH-PA Author Manuscript

NIH-PA Author Manuscript

NIH-PA Author Manuscript

command. Peak current amplitude at +40 mV: Control: +38.7 ± 3.4 pA/pF; $n = 14$. Cx43D378stop: +29.1 ± 2.1 pA/pF; $n = 15$, $P < 0.03$. **f** Current densities of three different outward current components at +40 mV. A1 ($I_{to,\ f}$): 23.5 ± 3.3 pA/pF for control and 15.5 ± 1.2 pA/pF for Cx43D378stop, $P < 0.04$; A2 ($I_{k,\ slow}$): 11.1 ± 0.9 pA/pF for control and 10.9 ± 1.6 pA/pF for Cx43D378stop (pNS); A0 (I_{ss}): 6.0 ± 0.5 pA/pF for control and 5.0 ± 0.6 pA/pF for Cx43D378stop (pNS)

NIH-PA Author Manuscript

NIH-PA Author Manuscript

NIH-PA Author Manuscript

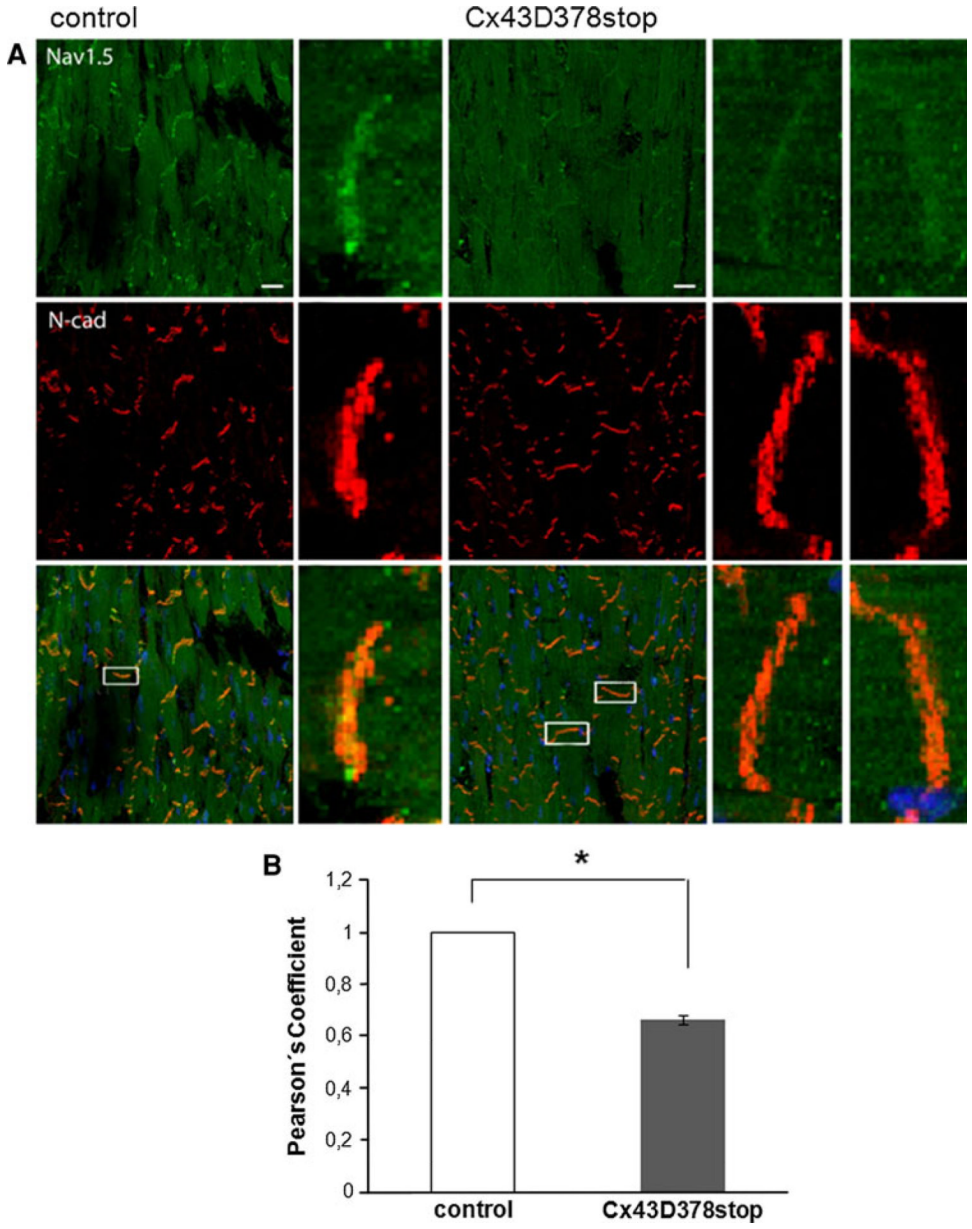

Fig. 6.

Localization of $Na_v1.5$ and N-Cadherin in adult Cx43D378stop hearts. **a** Immunological staining of $Na_v1.5$ (*green*), N-Cadherin (*red*) and nuclei (*blue*) shows co-localization of $Na_v1.5$ and N-Cadherin at intercalated discs between ventricular cardiomyocytes in sections of control and Cx43D378stop:αMyHC-Cre-ER(T2) hearts (merged magnifications, 63×). Bar: 20 μm. **b** Statistical evaluation (Pearson's coefficient) reveals a significantly reduced co-localization (~33 %) of $Na_v1.5$ and N-Cadherin at intercalated discs of Cx43D378stop hearts. Data are mean ± SEM of 158 intercalated discs analyzed for control and 393 for Cx43D378stop hearts

NIH-PA Author Manuscript
NIH-PA Author Manuscript
NIH-PA Author Manuscript

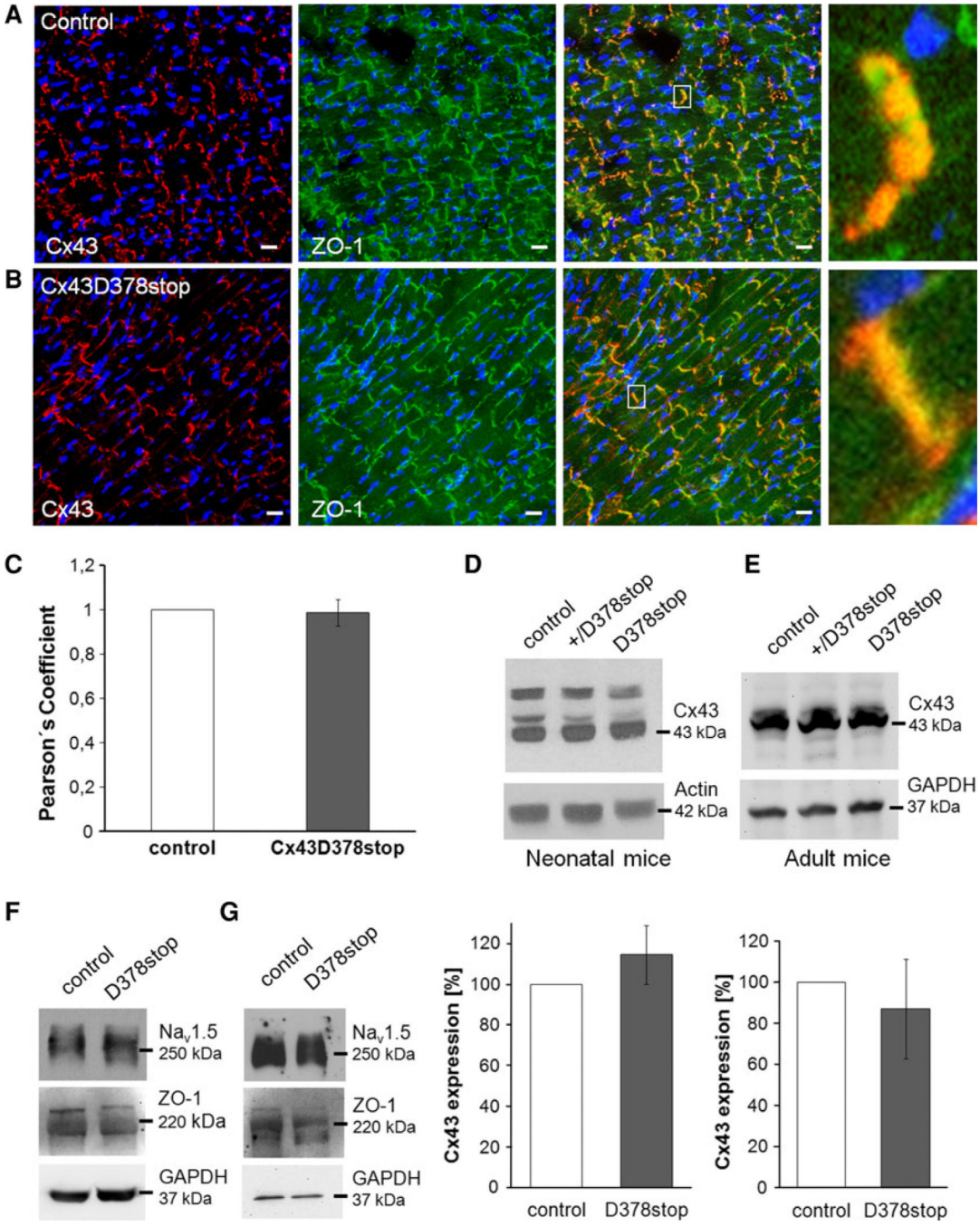

Fig. 7.

Expression and localization of mutated Cx43D378stop protein, ZO-1 and $Na_v1.5$ in the heart. Immunological staining of Cx43 (red), ZO-1 (*green*) and nuclei (*blue*) in sections of control (**a**) and Cx43D378stop hearts (**b**) verifies expression and membrane insertion of mutated Cx43D378stop protein. No obvious alterations in gap junction plaque formation or size were found for the Cx43D378stop protein. Cx43 and Cx43D378stop proteins both co-localized with ZO-1 at intercalated discs between ventricular cardiomyocytes (merged magnifications, 100×). Bar 20 μm. **c** Statistical evaluation (Pearson's coefficient) revealed no significant difference in the colocalization of Cx43 and ZO-1 between control and

NIH-PA Author Manuscript

NIH-PA Author Manuscript

NIH-PA Author Manuscript

Cx43D378stop hearts. Data are mean ± SEM of 147 intercalated discs analyzed for control and 165 for Cx43D378stop hearts. Western blot expression analyses showed no significant changes in Cx43 protein expression in newborn (**d**) and adult (**e**) Cx43D378stop hearts compared to controls. Equal levels of ZO-1 and $Na_V1.5$ protein in neonatal (**f**) and adult (**g**) Cx43D378stop hearts were detected in both groups. Blots were reprobed with actin- or GAPDH-antibodies to verify equal loading. $n = 4$ per group